

Amplitude and Phase of Spin-Echo Signals in Bulk Metals

D. Kotzur, M. Mehring, and O. Kanert

Institut für Physik der Universität Dortmund

(Z. Naturforsch. **28a**, 1607–1612 [1973]; received 18 July 1973)

The amplitude and phase of the spin echo signal in bulk metallic material after a $\beta_{10}-\tau-\beta_{20}(\alpha)$ pulse sequence has been calculated in the case of spin $I=3/2, 5/2, 7/2, 9/2$, for different ratios of the sample thickness to the skin depth. Optimal values for β_{10} , β_{20} and α are obtained in the sense that the echo signal is maximized. These optimal values depend again on the spin I and the relative sample size. The theoretical results compare reasonably well with experiments, performed on ^{63}Cu in copper foils of different size.

I. Introduction

NMR in metals has attracted much attention during the last two decades of NMR history. Since the skin effect leads to an attenuation and phase shifting of the applied rf-field, the cw NMR signal is a linear combination of the absorption and the dispersion part of the nuclear susceptibility, where the coefficients depend on the sample size relative to the skin depth^{1, 2}. Although the absorption and dispersion part of the signal can be disentangled due to the Kramers-Kronig relation³, most NMR measurements are done in powdered samples or very thin foils, where the observed signal corresponds, to the absorption part.

However, there is considerable interest in the study of bulk metallic specimens, like thick foils and single crystals, when anisotropies and lattice distortions are important^{4–9}. We have shown recently^{10, 11}, that the amplitude and phase of the Bloch decay in a metallic sample depends strongly on the relative sample size with respect to the skin depth. — From this it follows, that proper phase setting of the reference phase of the pulse spectrometer, as given by the values φ of Refs.^{10, 11} leads to a Bloch decay, whose Fourier transformation results in a true absorption signal.

We wish to elaborate in this paper on the influence of the skin effect on the amplitude and phase of the spin echo signal, produced by a $\beta_{10}-\tau-\beta_{20}(\alpha)$ pulse sequence, where β_{10} , β_{20} are the rotation angles of the two rf pulses at the surface of the sample and α is their phase difference.

Reprint requests to Prof. Dr. O. Kanert, Lehrstuhl für Experimentelle Physik III der Universität Dortmund, D-4600 Dortmund-Eichlinghofen, Baroper Straße.

II. Echo Formation by a $\beta_{10}-\tau-\beta_{20}(\alpha)$ Sequence

Due to the skin effect, the H_1 -field during rf irradiation is attenuated and phase shifted gradually, when penetrating into the sample. In the case of a metallic plate of thickness d , the H_1 -field parallel to the surface, can be expressed as¹¹

$$H_1(s) = H_{10} K(s) e^{i\Phi(s)} \quad (1)$$

with

$$K^2(s) = \frac{\sinh^2 s + \cos^2 s}{\sinh^2 c + \cos^2 c} \quad (1\text{ a})$$

and

$$\Phi(s) = \arctan \frac{\tanh s \tan s - \tanh c \tan c}{1 + \tanh s \tan s \tanh c \tan c} \quad (1\text{ b})$$

and where H_{10} is the rf field at the surface of the sample.

Here

$$s = x/\delta$$

is the relative coordinate of a spin with respect to the skin depth δ , where the origin is at the center of the plate and where

$$c = d/2 \delta.$$

Figure 1 shows the amplitude $K(s)$ and phase $\Phi(s)$ of the rf field at different positions in the sample, for different values of the relative sample thickness c .

Let us consider the following Hamiltonian in the rotating frame on resonance

$$\mathcal{H} = \mathcal{H}_p + \mathcal{H}_{\text{int}} \quad (2)$$

where \mathcal{H}_p represents the Hamiltonian due to the rf pulse and where the interaction may be represented by a quadrupolar part and an inhomogeneous line broadening as follows¹²

$$\mathcal{H}_{\text{int}} = b \hbar I_z + a \hbar \cdot (I_z^2 - \frac{1}{3} I^2) \quad (3)$$



Dieses Werk wurde im Jahr 2013 vom Verlag Zeitschrift für Naturforschung in Zusammenarbeit mit der Max-Planck-Gesellschaft zur Förderung der Wissenschaften e.V. digitalisiert und unter folgender Lizenz veröffentlicht: Creative Commons Namensnennung-Keine Bearbeitung 3.0 Deutschland Lizenz.

Zum 01.01.2015 ist eine Anpassung der Lizenzbedingungen (Entfall der Creative Commons Lizenzbedingung „Keine Bearbeitung“) beabsichtigt, um eine Nachnutzung auch im Rahmen zukünftiger wissenschaftlicher Nutzungsformen zu ermöglichen.

This work has been digitized and published in 2013 by Verlag Zeitschrift für Naturforschung in cooperation with the Max Planck Society for the Advancement of Science under a Creative Commons Attribution-NoDerivs 3.0 Germany License.

On 01.01.2015 it is planned to change the License Conditions (the removal of the Creative Commons License condition "no derivative works"). This is to allow reuse in the area of future scientific usage.

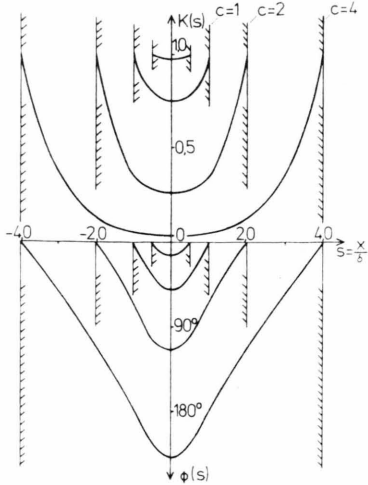


Fig. 1. Amplitude $K(s)$ and phase $\Phi(s)$ of the rf field H_1 inside a metallic plate for different sample size c .

with the quadrupole frequency

$$a = 3 e Q V_{zz} / 4 I (2 I - 1) \hbar$$

(Q : nuclear quadrupole moment, V_{zz} : z-component of the EFG tensor)³, and the “broadening frequency” b .

The corresponding frequency distributions are assumed to be normalized

$$\int_{-\infty}^{+\infty} db g_D(b) = \int_{-\infty}^{+\infty} da g_Q(a) = 1 \quad (4)$$

and symmetric with respect to $a = b = 0$.

The Hamiltonian of the rf pulse \mathcal{H}_p can be expressed as

$$\mathcal{H}_p = -\gamma \hbar H_{10} K(I_y \cos \Phi - I_x \sin \Phi)$$

where insertion of $H_1(s)$ according to Eq. (1) with irradiation in the y -direction of the rotating frame yields:

$$\mathcal{H}_p = -\gamma \hbar H_{10} K(I_y \cos \Phi - I_x \sin \Phi). \quad (5)$$

In evaluating the echo signal at $t = 2\tau$ with $\tau \ll T_2$, where τ is the spacing of the two applied rf pulses, we follow here the same procedures as outlined in Refs.^{12, 13} with the modifications due the skin effect. Assuming the rf field always strong compared with the other nuclear interactions we may express the spin density matrix at times $t \geq 2\tau$ using the δ -pulse approximation as

$$\varrho(t - 2\tau) = L(t) \varrho(0) L^{-1}(t) \quad (6)$$

where

$$L(t) = U(t, \tau) \cdot R_{\beta_1} \cdot U(\tau, 0) R_{\beta_2} \quad (7)$$

with

$$U(t_2, t_1) = \exp\{(-i/\hbar) \mathcal{H}_{\text{int}}(t_2 - t_1)\}, \quad (8)$$

$$R_{\beta_k} = \exp\{(-i/\hbar) \mathcal{H}_{\text{pk}} \cdot t_{\text{pk}}\} \quad k = 1, 2 \quad (9)$$

and where $\varrho(0)$ may be expressed as $\varrho(0) = C I_z$ ¹¹.

Equation (9) leads for the first pulse ($k = 1$), where the rf field is assumed to be applied in the y -direction to

$$R_{\beta_1} = \exp\{-i \Phi I_z\} \exp\{i \beta_1 I_y\} \exp\{i \Phi I_z\} \quad (10)$$

whereas for the second pulse ($k = 2$) a phase shift α of the rf field with respect to the first pulse is assumed

$$R_{\beta_2} = \exp\{-i \alpha I_z\} \exp\{-i \Phi I_z\} \exp\{i \beta_2 I_y\} \cdot \exp\{i \Phi I_z\} \exp\{i \alpha I_z\} \quad (11)$$

where

$$\beta_{1,2} = K(s) \cdot \gamma \cdot H_{10} \cdot t_{\text{p1,2}} = K(s) \cdot \beta_{10,20}. \quad (12)$$

Thus β_{10} and β_{20} are the rotation angles of the spins at the surface. The expectation values of I_{\pm} at times $t \geq 2\tau$ for the different spins at the location s in the sample can now be expressed, using

$$\langle I_+ \rangle = \text{Tr}\{\varrho(t - 2\tau) I_+\} \quad (13)$$

and following the same lines as in Ref.¹³ as:

$$\langle I_+ \rangle = C e^{i\Phi} \sum_{m, m'} [I(I+1) - m(m+1)]^{1/2} (-1)^{m-m'} m' d_{m, m+1}^2(\beta_2) d_{m+1, m'}(\beta_1) d_{m', m}(\beta_1) \cdot \exp\{i(t - 2\tau) ((2m+1)a + b)\} \quad (14)$$

where the rotation matrices

$$d_{m, m'}(\beta) = \langle m | \exp\{-i \beta I_y\} | m' \rangle \quad (15)$$

and their symmetry relations have been used¹⁴.

The rf magnetization proportional to $\langle I_+ \rangle$ at the locations of the spin, is again attenuated and phase shifted on its way to the surface in the same fashion as described by Equation (1). Thus the voltage induced in the probe coil by the magnetization, coming from the spins at location s is proportional to

$$\langle \tilde{I}_+(t - 2\tau) \rangle = K(s) e^{i\Phi(s)} \langle I_+(t - 2\tau) \rangle. \quad (16)$$

Introducing the echo signal $\tilde{E}_+(t - 2\tau)$ which is normalized to the total magnetization $\langle I_z \rangle$

$$\tilde{E}_+(t - 2\tau) = \langle \tilde{I}_+(t - 2\tau) \rangle / \langle I_z \rangle \quad (17)$$

belonging to nuclei with the same set of (a, b, s) values, the observed echo signal of the whole sample

can be expressed as

$$E_+(t-2\tau) = \int_0^c ds \int_{-\infty}^{+\infty} da \int_{-\infty}^{+\infty} db \tilde{E}_+(t-2\tau) g_Q(a) g_D(b). \quad (18)$$

From Eq. (18) the magnetization in the x - and

y -direction can be calculated, using:

$$E_x(t') = \frac{1}{2} (E_+(t-2\tau) + E_+^*(t-2\tau)) \quad (19)$$

and

$$E_y(t') = (1/2i) (E_+(t-2\tau) - E_+^*(t-2\tau)) \quad (20)$$

where E_+^* denotes the complex conjugate of E_+ .

As the result we obtain:

$$E_x(t') = A_{-1/2}^I \cdot D(t') + \sum_{m=1/2}^{I-1} 2 \cdot A_m^I \cdot D(t') \cdot Q^{(m)}(t'), \quad (21)$$

$$E_y(t') = B_{-1/2}^I \cdot D(t') + \sum_{m=1/2}^{I-1} 2 \cdot B_m^I \cdot D(t') \cdot Q^{(m)}(t') \quad (22)$$

where the coefficients A_m^I and B_m^I are given by

$$A_m^I = \frac{3[I(I+1) - m(m+1)]^{1/2}}{I(I+1)(2I+1)} \sum_{m'} m' (-1)^{m'-m} \int_0^c K d_{m,m+1}^2(\beta_2) \cdot d_{m+1,m'}(\beta_1) \cdot d_{m',m}(\beta_1) \cdot \cos(2\Phi + 2\alpha) ds, \quad (23)$$

$$B_m^I = \frac{3[I(I+1) - m(m+1)]^{1/2}}{I(I+1)(2I+1)} \sum_{m'} m' (-1)^{m'-m} \int_0^c K d_{m,m+1}^2(\beta_2) \cdot d_{m+1,m'}(\beta_1) \cdot d_{m',m}(\beta_1) \cdot \sin(2\Phi + 2\alpha) ds. \quad (24)$$

The function $D(t')$ and $Q^{(m)}(t')$ are Fourier transforms of the corresponding distribution function $g_D(b)$ and $g_Q(a)$, respectively:

$$D(t') = \int_{-\infty}^{+\infty} g_D(b) \cos(bt') db \quad (25)$$

$$Q^{(m)}(t') = Q((2m+1)t') = \int_{-\infty}^{+\infty} g_Q(a) \cos((2m+1)at') da. \quad (26)$$

With $t' = 0$ i.e. $t = 2\tau$, and $D(0) = Q^{(m)}(0) = 1$, a short hand notation of the echo signal is obtained as:

$$E_x(0) = E_{Mx} + E_{Sx} \quad (27)$$

and

$$E_y(0) = E_{My} + E_{Sy} \quad (28)$$

where

$$E_{Mx} = A_{-1/2}^I, \quad (29)$$

$$E_{My} = B_{-1/2}^I, \quad (30)$$

$$E_{Sx} = \sum_{m=1/2}^{I-1} 2 A_m^I, \quad (31)$$

$$E_{Sy} = \sum_{m=1/2}^{I-1} 2 B_m^I. \quad (32)$$

Using Eqs. (23), (24), (29) to (32) it is possible to calculate the echo amplitudes for every set of the values β_{10} , β_{20} , α , c . However this is not very usefull, since one is mainly interested in ob-

taining maximum signal height. Thus we optimized by numerical computer calculations the echo height, with respect to the parameters β_{10} and α . The values for which maximum signal height is obtained are denoted $\beta_{10}^{(opt)}$ and α_{opt} .

Figures 2 show the dependence of α_{opt} and $\beta_{10}^{(opt)}$ on the relative sample size c .

There are some interesting features of α_{opt} and $\beta_{10}^{(opt)}$ which we would like to mention:

- α_{opt} and $\beta_{10}^{(opt)}$ are same for all spins I .
- The same value of $\beta_{10}^{(opt)}$ which maximizes the echo amplitude, gives a maximum amplitude of the Bloch decay¹¹.
- A simple relation between α_{opt} and the phase φ_{opt} of the Bloch decay signal holds, i.e.

$$\alpha_{opt} = (90 - \varphi_{opt})/2. \quad (33)$$

In order to demonstrate the behavior of the echo signal for bulk metallic samples ($c \gg 0,5$) on the rotation angle β_{20} of the second rf pulse, with

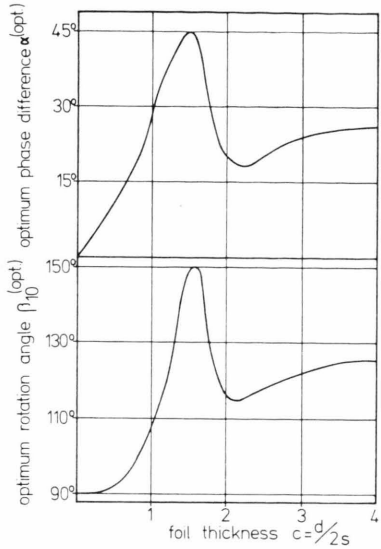


Fig. 2. Optimum phase difference $\alpha^{(\text{opt})}$ between the first and second rf pulse and optimum rotation angle $\beta_{10}^{(\text{opt})}$ of the first pulse as a function of the relative sample thickness $c = b/2\delta$. Note, that the values are independent of spin I .

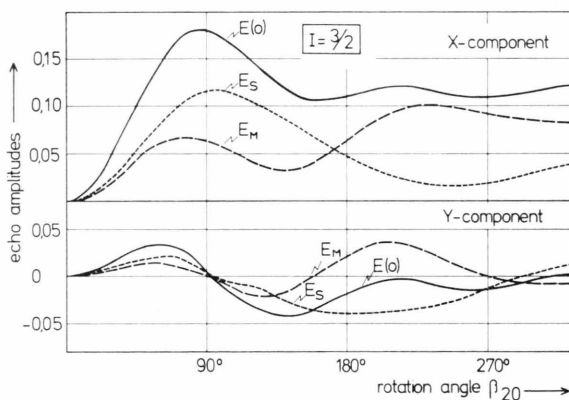


Fig. 3 a

the given initial condition $\beta_{10}^{(\text{opt})}$ and $\alpha^{(\text{opt})}$, in Fig. 3 the different contributions of the main transition (E_M) and the satellite transitions (E_S) to the total echo signal are plotted versus β_{20} . Notice that an angle $\beta_{20}^{(\text{opt})}$ can be defined, where a maximum echo signal is obtained in the x -direction, whereas the signal in the y -direction vanishes.

The effect of the relative sample size c on the echo amplitudes is demonstrated in Fig. 4 in the case of spin $I = 5/2$ only. If $c \leq 0.5$ the same behavior as obtained in ionic crystals¹³ is approached. In this case E_y vanishes.

Figure 5 shows the dependence of the different contributions E_M and E_Q to the echo signal versus β_{20} for a spin $I = 3/2$, according to the theory, derived above, for different sample size c . The experimental points plotted in Fig. 5 are obtained from ⁶³Cu resonance in copper foils of different thickness, according to the labelled c values, doped

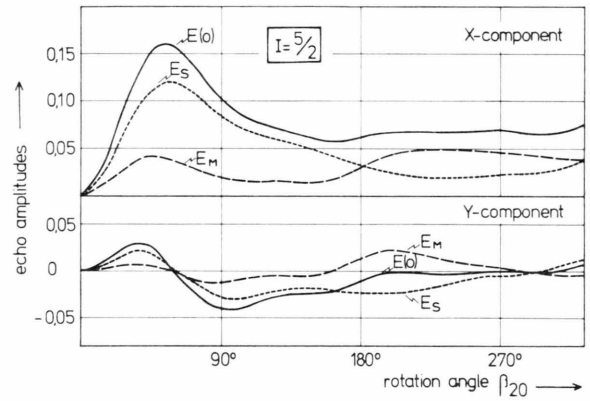


Fig. 3 b

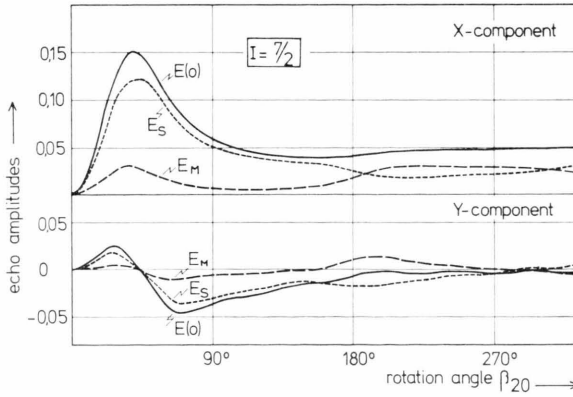


Fig. 3 c

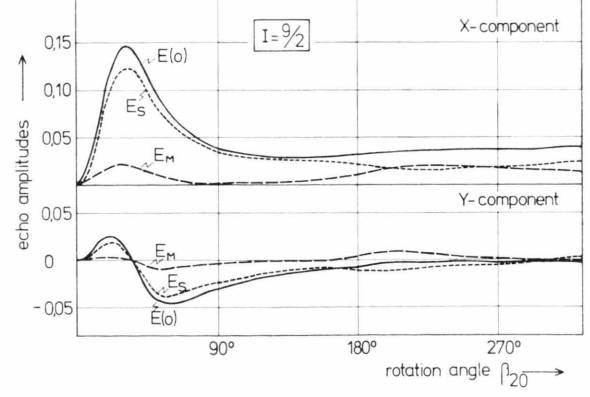


Fig. 3 d

Fig. 3. x -component and y -component of the amplitudes of the main transition (E_M), of the satellite transition (E_S) and of the total signal $E(0) = E_M + E_S$ versus the second rotation angle β_{20} for the optimum values $\beta_{10}^{(\text{opt})}$, $\alpha^{(\text{opt})}$ in the case of bulk metals ($c \geq 0.5$) spin $I = 3/2$ (a), $5/2$ (b), $7/2$ (c), $9/2$ (d).

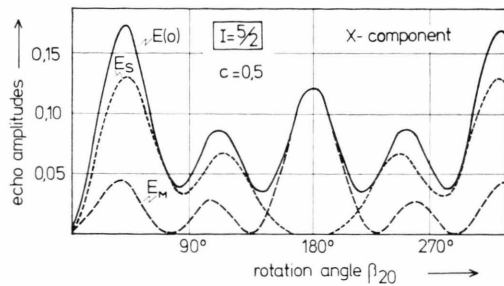


Fig. 4 a

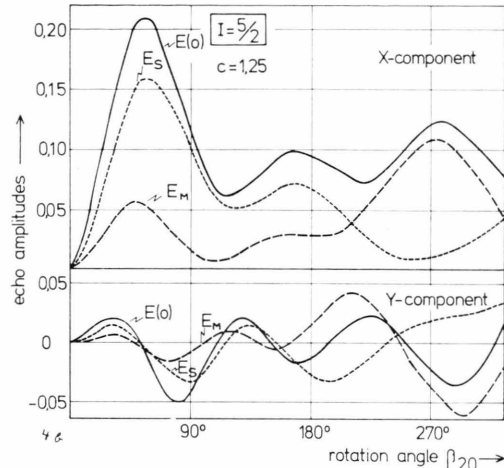


Fig. 4 b

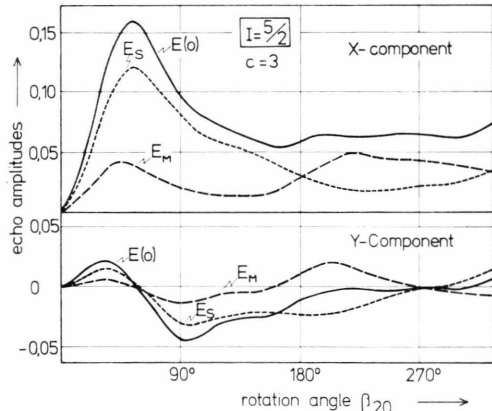


Fig. 4 c

Fig. 4. Same as in Fig. 3 except that the parameter is the relative sample thickness c : $c=0.5$ (a), $c=1.25$ (b), $c=3$ (c) (spin $I=5/2$). Note, that in the case of $c \leq 0.5$ the E_y -component vanishes.

with 3.2 at % Sn. The measurements were performed at 16.058 MHz, (skin depth of the doped material: 21μ) using a Bruker pulse spectrometer

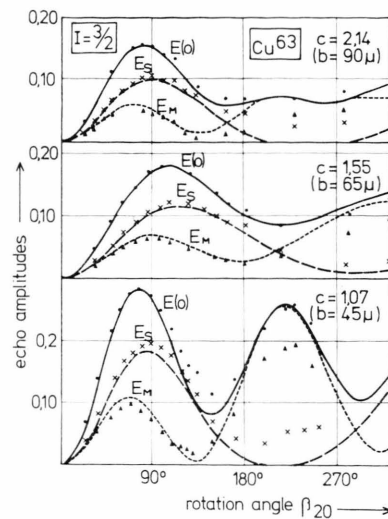


Fig. 5. Plot of the theoretical components of the echo amplitudes $[E_M, E_S, E(0)]$ (lines) and experimental data (dots) obtained from the Cu^{63} echo in doped copper versus β_{20} , with the settings $\beta_{10} = \beta_{10}^{(\text{opt})}$ and $\alpha = \alpha^{\text{opt}}$. Parameter: sample thickness.

SXP 4-60. The strong doping of the copper material results in a considerable quadrupole distortion, which shows up as a drastic decrease in the width of the satellite part E_S , which can thus be easily distinguished from the main transition E_M as shown previously¹³. A line shape analysis of the quadrupolar part of the echo due to these point defects will be described in a different paper¹⁵. Since the above theory is valid only for $\tau \ll T_2$, the echo amplitudes are determined for various τ values and extrapolated to $\tau = 0$.

There is considerable agreement between theory and experiment up to $\beta_{20} = 180^\circ$. For larger β_{20} values, errors due to H_1 field inhomogeneity, receiver blocking time and the invalidity of the δ pulse approximation affect the echo amplitude.

It can be summarized, that maximum echo signal is obtained for

$$\beta_{10}^{(\text{opt})} = 124^\circ; \alpha_{\text{opt}} = 28^\circ$$

in the case of bulk material ($c \gg 1$) independent of spin I . The value of $\beta_{20}^{(\text{opt})}$, however, depends on I as shown in Table 1. Since E_y vanishes for $\beta_{20} = \beta_{10}^{(\text{opt})}$ as shown above, it is convenient for practical purposes to normalize $E_x(t)$, so that

$$E_x(0) = 1.$$

Table 1

Spin I	3/2	5/2	7/2	9/2
$\beta_{20}^{(opt)}$	87°	55°	41°	33°
$C_{-1/2}$	0.367	0.249	0.190	0.153
$2 C_m$				
$m = 1/2$	0.633	0.466	0.361	0.295
$m = 3/2$	—	0.285	0.297	0.265
$m = 5/2$	—	—	0.152	0.199
$m = 7/2$	—	—	—	0.088
C_s	0.633	0.751	0.810	0.847

This leads to

$$E_n(t) = C_{-1/2} D(t) + \sum_{m=1/2}^{I-1} 2 C_m \cdot D(t) Q^{(m)}(t) \quad (34)$$

or

$$E_n(t) = C_{-1/2} \cdot D(t) + C_s \cdot D(t) \cdot Q^+(t) \quad (35)$$

- ¹ N. Bloembergen, J. Appl. Phys. **23**, 1383 [1952].
- ² A. C. Chapman, R. Rhodes, and E. F. Seymour, Proc. Phys. Soc. London **B 70**, 345 [1957].
- ³ P. L. Sagalyn and J. A. Hofmann, Phys. Rev. **127**, 68 [1962].
- ⁴ E. P. Jones and D. L. Williams, Cand. J. Phys. **42**, 1499 [1964].
- ⁵ L. E. Drain, Met. Rev. **12**, 195 [1967].
- ⁶ R. W. Weinert and R. T. Schumacher, Phys. Rev. **172**, 711 [1968].
- ⁷ O. Kanert, Phys. Stat. Sol. **32**, 667 [1969].
- ⁸ H. E. Schone, Phys. Rev. **183**, 410 [1969].
- ⁹ O. Kanert and K. Preußer, Phys. Stat. Sol. (a) **15**, 483 [1973].

where

$$C_m = A^I m \quad \left| \sum_{m=1/2}^{I-1} A^I m \right., \quad (36)$$

$$C_s = \sum_{m=1/2}^{I-1} 2 C_m, \quad (37)$$

and

$$Q^+(t) = \sum_{m=1/2}^{I-1} \frac{2 C_m}{C_s} Q^{(m)}(t). \quad (38)$$

The coefficients C are listed in Table 1 in the case of bulk material ($c \gg 1$) and are essentially the same as the ones obtained in the case of ionic solids¹².

- ¹⁰ M. Mehring, D. Kotzur, and O. Kanert, Phys. Stat. Sol. (b) **53**, K 25 [1972].
- ¹¹ D. Kotzur, O. Kanert, and M. Mehring, Proceeding of the 17th Colloque Ampere (Turku 1972), North-Holland Publishing Company (in press).
- ¹² O. Kanert and M. Mehring, Static Quadrupole Effects in Disordered Cubic Solids, NMR-Basic Principles and Progress, Vol. III, Springer-Verlag, Heidelberg 1971.
- ¹³ M. Mehring and O. Kanert, Z. Naturforsch. **24a**, 768 [1969].
- ¹⁴ D. M. Brink and G. R. Satchler, Angular Momentum, Clarendon Press, Oxford 1968.
- ¹⁵ O. Kanert, D. Kotzur, and M. Mehring, Sol. Stat. Com. [1973], to be published.